

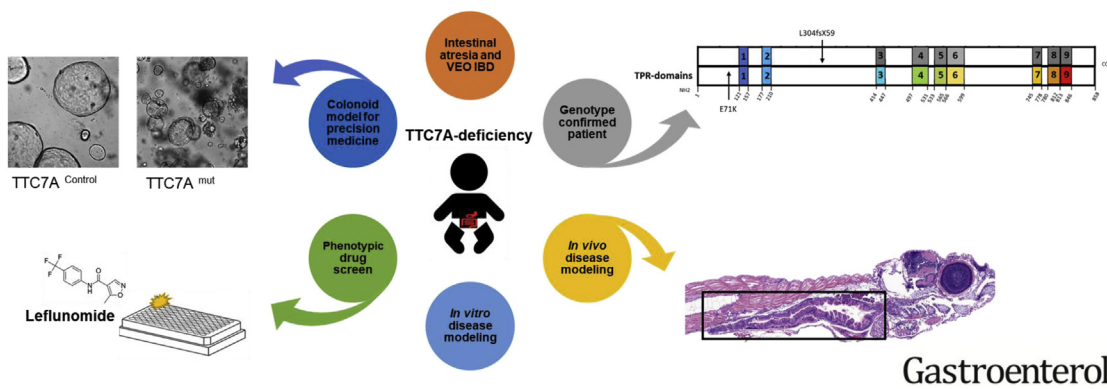


Drug Screen Identifies Leflunomide for Treatment of Inflammatory Bowel Disease Caused by TTC7A Deficiency

Sasha Jardine,¹ Sierra Anderson,^{2,3} Stephen Babcock,^{2,3} Gabriella Leung,¹ Jie Pan,¹ Neel Dhingani,¹ Neil Warner,¹ Conghui Guo,¹ Iram Siddiqui,⁴ Daniel Kotlarz,⁵ James J. Dowling,^{6,7} Roman A. Melnyk,⁷ Scott B. Snapper,^{2,3,8} Christoph Klein,⁵ Jay R. Thiagarajah,^{2,3} and Aleixo M. Muişe^{1,9,10}

¹SickKids Inflammatory Bowel Disease Centre, The Hospital for Sick Children, Toronto, Ontario, Canada; ²Division of Gastroenterology, Hepatology and Nutrition, Boston Children's Hospital, Boston, Massachusetts; ³Harvard Medical School, Boston, Massachusetts; ⁴Division of Pathology, The Hospital for Sick Children, Toronto, Ontario, Canada; ⁵Dr von Hauner Children's Hospital, Department of Pediatrics, University Hospital, Ludwig Maximilian University Munich, Munich, Germany; ⁶Division of Neurology, and Genetics and Genome Biology Program, Research Institute, The Hospital for Sick Children, Toronto, Ontario, Canada; ⁷Molecular Medicine Program, Research Institute, The Hospital for Sick Children, Toronto, Ontario, Canada; ⁸Division of Gastroenterology, Brigham and Women's Hospital, Boston, Massachusetts; ⁹Cell Biology Program, Research Institute, The Hospital for Sick Children, Toronto, Ontario, Canada; and ¹⁰Department of Pediatrics, Institute of Medical Science and Biochemistry, University of Toronto, The Hospital for Sick Children, Toronto, Ontario, Canada

Drug screen identifies leflunomide for the treatment of inflammatory bowel disease caused by TTC7A deficiency



BACKGROUND & AIMS: Mutations in the tetratricopeptide repeat domain 7A gene (*TTC7A*) cause intestinal epithelial and immune defects. Patients can become immune deficient and develop apoptotic enterocolitis, multiple intestinal atresia, and recurrent intestinal stenosis. The intestinal disease in patients with *TTC7A* deficiency is severe and untreatable, and it recurs despite resection or allogeneic hematopoietic stem cell transplant. We screened drugs for those that prevent apoptosis of in cells with *TTC7A* deficiency and tested their effects in an animal model of the disease. **METHODS:** We developed a high-throughput screen to identify compounds approved by the US Food and Drug Administration that reduce activity of caspases 3 and 7 in *TTC7A*-knockout (*TTC7A*-KO) HAP1 (human haploid) cells and reduce the susceptibility to apoptosis. We validated the effects of identified agents in HeLa cells that stably express *TTC7A* with point mutations found in patients. Signaling pathways in cells were analyzed by immunoblots. We tested the effects of identified agents in zebrafish with disruption of *ttc7a*, which develop intestinal defects, and colonoids derived from

biopsy samples of patients with and without mutations in *TTC7A*. We performed real-time imaging of intestinal peristalsis in zebrafish and histologic analyses of intestinal tissues from patients and zebrafish. Colonoids were analyzed by immunofluorescence and for ion transport. **RESULTS:** *TTC7A*-KO HAP1 cells have abnormal morphology and undergo apoptosis, due to increased levels of active caspases 3 and 7. We identified drugs that increased cell viability; leflunomide (used to treat patients with inflammatory conditions) reduced caspase 3 and 7 activity in cells by 96%. *TTC7A*-KO cells contained cleaved caspase 3 and had reduced levels of phosphorylated AKT and X-linked inhibitor of apoptosis (XIAP); incubation of these cells with leflunomide increased levels of phosphorylated AKT and XIAP and reduced levels of cleaved caspase 3. Administration of leflunomide to *ttc7a*^{-/-} zebrafish increased gut motility, reduced intestinal tract narrowing, increased intestinal cell survival, increased sizes of intestinal luminal spaces, and restored villi and goblet cell morphology. Exposure of patient-derived colonoids to leflunomide increased cell survival,

polarity, and transport function. **CONCLUSIONS:** In a drug screen, we identified leflunomide as an agent that reduces apoptosis and activates AKT signaling in TTC7A-KO cells. In zebrafish with disruption of *ttc7a*, leflunomide restores gut motility, reduces intestinal tract narrowing, and increases intestinal cell survival. This drug might be repurposed for treatment of TTC7A deficiency.

Keywords: Genetic; Monogenic IBD; Animal Model; Cell Death.

Biallelic mutations in tetratricopeptide repeat domain 7A (*TTC7A*) result in a combined primary intestinal epithelial and immune defect that presents clinically as immunodeficiency, very-early-onset inflammatory bowel disease (IBD) and/or multiple intestinal atresia.¹⁻³ Since 2013, there have been >50 reported cases of *TTC7A* deficiency, with two thirds of affected children dying within the first 12 months of life.³⁻⁵ Children with *TTC7A* deficiency present with severe multisystemic disease, including apoptotic enterocolitis (ie, intestinal inflammation arising from elevated intestinal epithelial cell apoptosis), friable and/or exfoliative mucosa, congenital intestinal atresia and recurrent stenosis, lymphocytopenia, and combined immunodeficiency. Poor response to standard treatment regimens, including steroids, surgery, and allogeneic hematopoietic stem cell transplant, as well as the recurrence of bowel disease and the high mortality rate in these patients,¹ motivated our expedited search for effective therapies to treat *TTC7A* deficiency.

TTC7A contains 9 tetratricopeptide repeat (TPR) domains, which are structural motifs found in a range of proteins typically associated with trafficking and scaffolding.⁶ Our group previously reported that *TTC7A* acts as a scaffolding protein by shuttling phosphatidylinositol 4-kinase-3 alpha (*PI4KIII α*) to the plasma membrane, where *PI4KIII α* catalyzes the synthesis of phosphatidylinositol 4-phosphate (*PI4P*) from phosphatidylinositol (PI) membrane lipids.¹ Homeostatic levels of anionic *PI4P* are important for plasma membrane identity, apicobasal polarity, cell survival, and production of poly-phosphorylated phosphatidylinositol phosphate lipids *PI (4,5)P₂/PI(3,4,5)P₃*.⁷ Plasma membrane *PI4P* synthesis is exclusively dependent on the function and localization of *PI4KIII α* . Mouse and zebrafish models have provided strong evidence for a relationship between *PI* homeostasis, *PI4KIII α* function, and intestinal health.^{8,9}

To accelerate viable treatment options for patients with *TTC7A* deficiency, we carried out a phenotypic high-throughput drug screen using a US Food and Drug Administration (FDA)-approved drug library and identified leflunomide, a disease-modifying antirheumatic drug,¹⁰ as a candidate therapeutic. In *TTC7A*-knockout (KO) cells, *ttc7a*-mutant zebrafish, and *TTC7A*-deficient patient-derived colonoids, we show that leflunomide rescues defective AKT signaling and improves multiple intestinal phenotypes. Our findings therefore support leflunomide as a candidate drug to move forward for further clinical studies.

WHAT YOU NEED TO KNOW

BACKGROUND AND CONTEXT

Mutations in the tetratricopeptide repeat domain 7A gene (*TTC7A*) cause intestinal epithelial and immune defects, apoptotic enterocolitis, multiple intestinal atresia, and recurrent intestinal stenosis.

NEW FINDINGS

In a drug screen, the authors identified leflunomide as an agent that reduces apoptosis and levels of active caspase 3 in *TTC7A*-knockout cells. In zebrafish with disruption of *ttc7a*, leflunomide restored gut motility, reduced intestinal tract narrowing, and increased intestinal cell survival.

LIMITATIONS

Further studies are needed in humans.

IMPACT

Leflunomide might be repurposed for treatment of *TTC7A* deficiency.

Materials and Methods


Cells and Drug Treatment

Generating an intestinal *TTC7A* knockout (*TTC7A*-KO) stable cell line was unsuccessful; thus, HAP1 (human haploid) cells were selected as our in vitro model because they were commercially available via Horizon Discovery (Cambridge, UK) and engineered using clustered regularly interspaced short palindromic repeats (CRISPR)/Cas9 genome editing. Drugs and concentrations included dimethyl sulfoxide (DMSO) (0.5% volume [vol]/vol), cyanocobalamin (10 μ mol/L) (Selleckchem, Houston, TX), leflunomide (4 μ mol/L) (Selleckchem), tiaprofenic acid (4 μ mol/L) (Prestwick Chemical Library; Illkirch, France), fenbufen (10 μ mol/L) (Selleckchem) fasudil (5 μ mol/L) (Selleckchem), Y27632 (10 μ mol/L) (Selleckchem), and 4-phenylbutyrate (4-PBA) (5 mmol/L) (Sigma-Aldrich, St. Louis, MO).

Western Blotting

Western blotting was completed as per standard protocols. Primary antibodies included anti-caspase 3 rabbit, anti-p-AKT (S473) rabbit anti-p-AKT (T308) rabbit monoclonal antibody, anti-AKT rabbit, anti-XIAP (D2Z8W) rabbit monoclonal antibody (all from Cell Signaling Technology, Danvers, MA).

Abbreviations used in this paper: 4-PBA, 4-phenylbutyrate; CK20, cytokeratin 20; CRISPR, clustered regularly interspaced short palindromic repeats; DHODH, dihydroorotate dehydrogenase; DMSO, dimethyl sulfoxide; dpf, days postfertilization; FDA, US Food and Drug Administration; *IC*₅₀, half maximal inhibitory concentration; KO, knockout; IB, intestinal bulb; IBD, inflammatory bowel disease; mGluR5, metabotropic glutamate receptor subtype 5; mut, mutant; NSAID, nonsteroidal anti-inflammatory drug; PI, phosphatidylinositol; PI3K, phosphatidylinositol 3-kinase; *PI4KIII α* , phosphatidylinositol 4-kinase-3 alpha; *PI4P*, phosphatidylinositol 4-phosphate; TNF, tumor necrosis factor; vol, volume; WT, wild type; XIAP, X-linked inhibitor of apoptosis protein.

 Most current article

© 2020 by the AGA Institute. Published by Elsevier Inc. This is an open access article under the CC BY-NC-ND license (<http://creativecommons.org/licenses/by-nc-nd/4.0/>).

0016-5085

<https://doi.org/10.1053/j.gastro.2019.11.019>

Caspase Activity Assay and High-Throughput Drug Screen

TTC7A-KO cells were screened with Prestwick, Tocriscreen (Bristol, UK), and Library of Pharmacologically Active Compounds (LOPAC) drug libraries at 8 $\mu\text{mol/L}$, 8 $\mu\text{mol/L}$, and 5 $\mu\text{mol/L}$ concentrations, respectively, at the SMART laboratory for high-throughput programs (Toronto, Ontario, Canada). Mean caspase activity of controls was plotted, and compounds that reduced caspase activity below 3 standard deviations of the wild-type (WT) control cells (hit threshold = $\mu_{\text{WT}} - 3\sigma$), providing a confidence limit of 99.73%, were selected as hits.¹¹ Concentration-response curves (40–0.04 $\mu\text{mol/L}$) and half maximal inhibitory concentration (IC_{50}) values were generated with GraphPad software (GraphPad Software, San Diego, CA).

Zebrafish *ttc7a*^{-/-} Model, Maintenance, Husbandry, and Drug Treatment

All protocols and procedures involving zebrafish were performed in accordance with Canadian Council on Animal Care guidelines. Mutant *ttc7a* strains were generated and maintained by the Zebrafish Core Facility at Sickkids' Peter Gilgan Centre for Research and Learning by using CRISPR/Cas9 mutagenesis, following previously described protocols.¹² Heterozygous (*ttc7a*^{+/-}) and homozygous (*ttc7a*^{+/+}) fish displayed normal and indistinguishable intestinal phenotypes (ie, size, structure and motility); thus, both served as healthy controls for comparison to *ttc7a*^{-/-} fish. Zebrafish were treated during the larval stage (3–7 days postfertilization ([dpf])). Drugs were dissolved directly into the water, resulting in final concentrations corresponding to those used in *in vitro* experiments: DMSO (0.5% vol/vol), cyanocobalamin (10 $\mu\text{mol/L}$), leflunomide (4 $\mu\text{mol/L}$), tiaprofenic acid (4 $\mu\text{mol/L}$), and fenbufen (10 $\mu\text{mol/L}$).

Peristalsis Assays

Peristalsis assays were adapted from Shi et al.¹³ See [Supplementary Methods](#) for more detail.

Immunofluorescence Histochemical Staining on Formalin-Fixed, Paraffin-Embedded Sections

Human tissues were fixed in 10% neutral buffered formalin, without methanol, and embedded in paraffin by using routine protocols. The use of human tissue samples was approved by the Research Ethics Board (Hospital for Sick Children), and comprehensive consent was obtained. Informed consent to participate in research was obtained, and a copy of the consent is available on the NEOPICS Web site (<http://www.neopics.org/study-documents.html>). Zebrafish samples were fixed at 7 dpf by zinc formalin and embedded with paraffin. See [Supplementary Methods](#) for more details.

Consent and TTC7A Patient Genotyping and Biopsy Immunofluorescence

Human subject research was carried out under a study protocol approved by the Boston Children's Hospital institutional review board under protocol IRB-P00000529. Targeted gene panel sequencing was carried out at Boston Children's Hospital, where a patient was identified with deleterious

biallelic mutation in TTC7A (211G>A→Glu71Lys and 911delT→Leu304Arg). Mutations were validated using CLIA-approved Sanger sequencing. Formalin-fixed stomach, duodenum, and colon biopsies were processed for standard H&E and immunofluorescence.

Patient-Derived Intestinal Colonoid Culture

Colonic biopsy samples were obtained and cultured with methods modified from Sato et al.¹⁴ Briefly, crypts were dissociated from colonic biopsy samples obtained from a patient with TTC7A mutation or from a healthy control individual. Isolated crypts were suspended in Growth Factor Reduced Phenol Red Free Matrigel (Corning, Corning, NY) and plated as 50- μL domes in a tissue culture-treated 24-well plates (Thermo Fisher Scientific, Waltham, MA) with growth factor (Wnt, R-spondin, noggin)-supplemented media (see [Supplementary Methods](#) for media composition). Colonoid cultures were passaged by removal of Matrigel with Cell Recovery Solution (Corning), mechanical dissociation of colonoids, and replating in Matrigel every 4 days.

Colonoid Survival Assay

TTC7A-deficient and healthy control colonoids were plated in Matrigel with human colonoid media containing Rho-kinase inhibitor Y27632. After establishment of colonoids, Y27632 was removed from the media, and the colonoids were treated with leflunomide (10 $\mu\text{mol/L}$ and 2.5 $\mu\text{mol/L}$ in DMSO), or vehicle control (DMSO). See [Supplementary Methods](#) for more detail.

Colonoid Polarity

TTC7A-deficient and healthy control colonoids were cultured with human colonoid media without Rho-kinase inhibitor Y27632 and with or without leflunomide (10 $\mu\text{mol/L}$). At 48 hours after plating, colonoids (50 per group) were visually assessed by 2 blinded investigators and counted for the presence of multiple lumens. See [Supplementary Methods](#) for colonoid immunocytochemistry and histology.

Colonoid Swelling Assay

Colonoid swelling after leflunomide (10 $\mu\text{mol/L}$), Rho-kinase inhibitor, or DMSO treatment was performed as previously described.¹⁵ Measurements of cell diameter and subsequent calculation of volume change (assuming a sphere) was facilitated by Image J (National Institutes of Health, Bethesda, MD).

Statistical Analysis

Data are presented as mean \pm standard deviation or standard error of the mean. Statistical significance was calculated by GraphPad Prism software, version 6.0 as a 2-tailed 1-way or 2-way analysis of variance (ANOVA), or unpaired Student *t* test. Statistical significance was established at $P < .05$.

Results

Disease Modeling in TTC7A-KO Cells

To develop an assay for the phenotypic correction of TTC7A, we obtained human haploid (HAP1) TTC7A-KO cells,

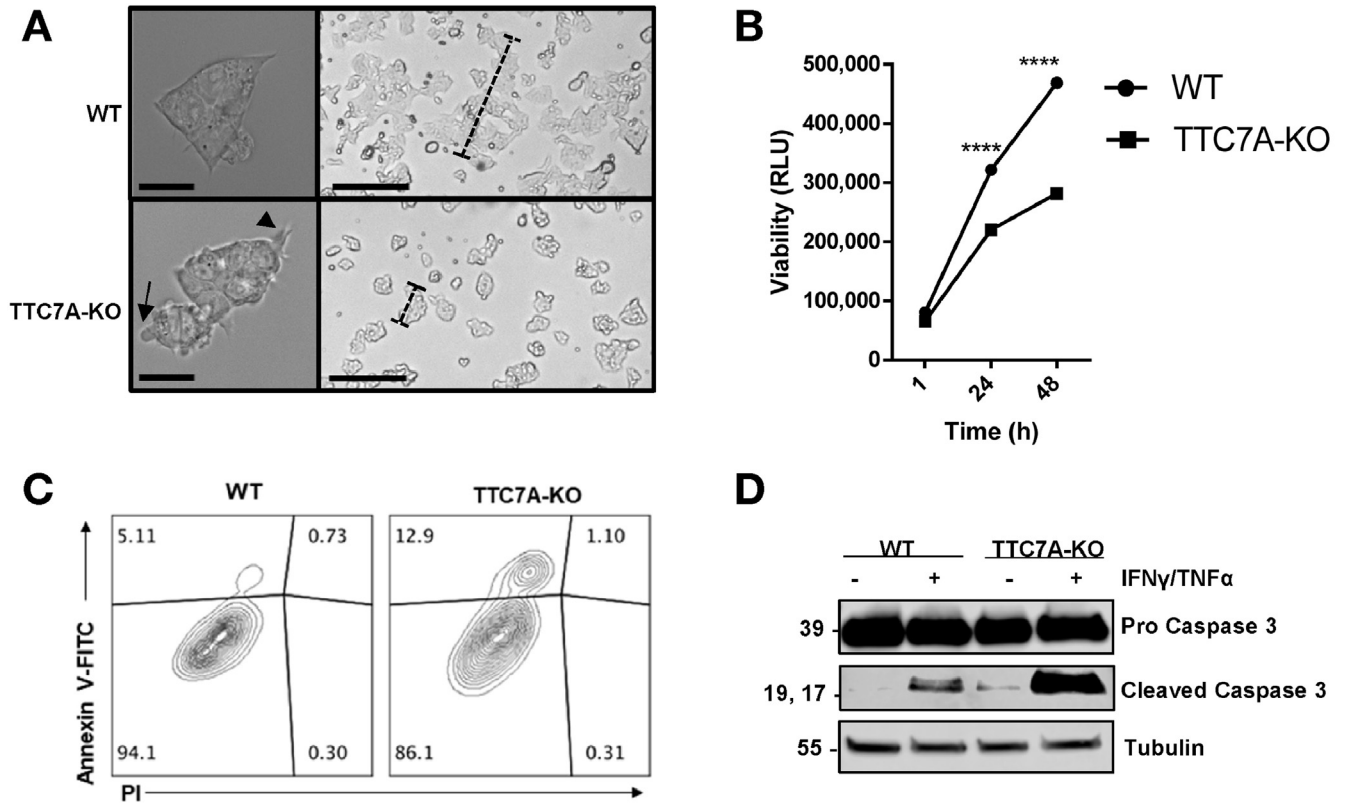


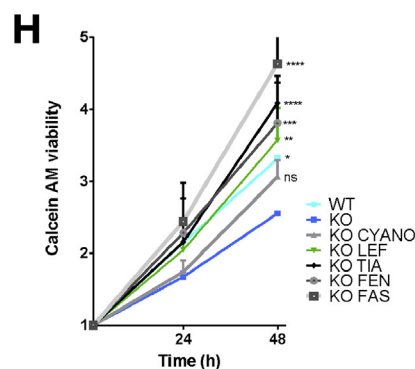
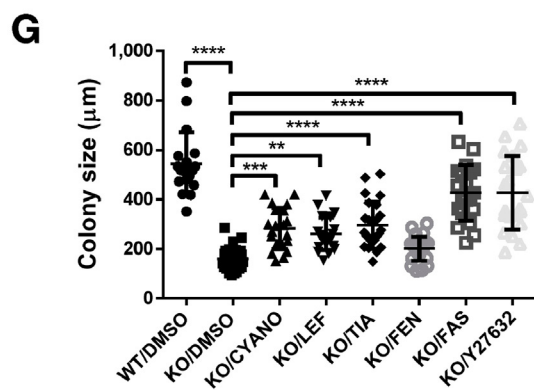
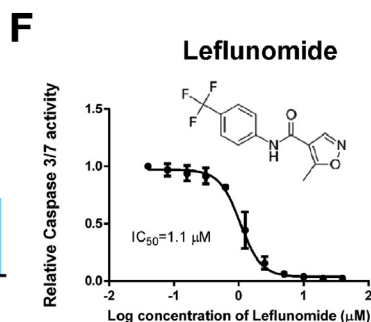
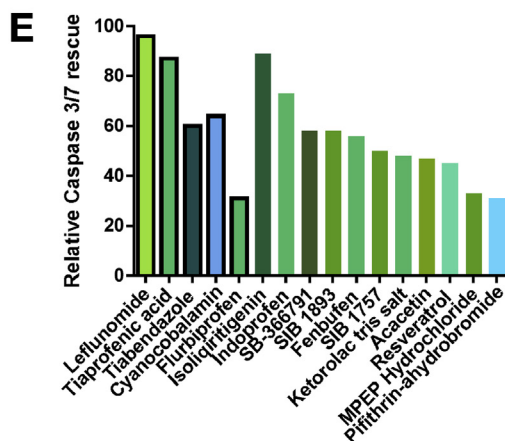
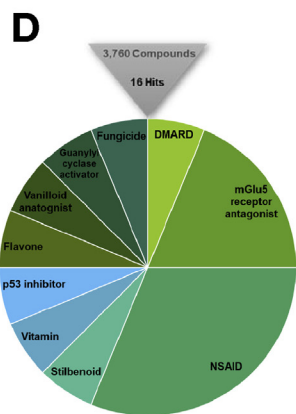
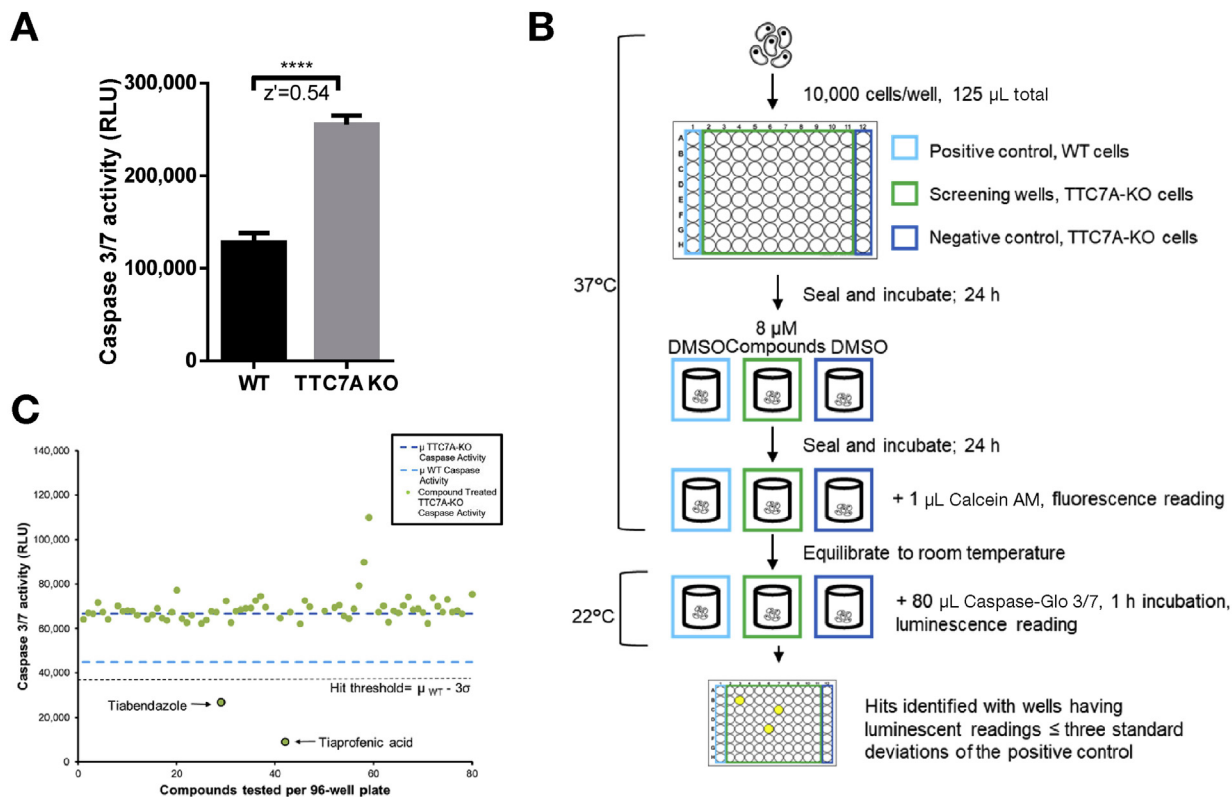
Figure 1. TTC7A-KO cells have an increased susceptibility for apoptosis. (A) Morphology of WT and TTC7A-KO HAP1 cells, differential interference contrast microscopy. The left panels show original objective magnification $\times 63$ (scale bar, $10 \mu\text{m}$). The right panels show original objective magnification $\times 4$ (scale bar, $190 \mu\text{m}$). Blebs and filopodia-like processes are indicated by the arrow and arrowhead, respectively. Dashed bars highlight differences in colony sizes after 48 hours of culturing. (B) Real-time viability assay. Two-way ANOVA with post hoc test (Sidak), **** $P < .0001$ ($n = 3$, 3 replicates). (C) Annexin V-fluorescein isothiocyanate/PI flow cytometry showed that TTC7A-KO cells have significantly increased annexin-V staining. Data are quantified in [Supplementary Figure 2B](#). (D) Western blot analysis of untreated and interferon gamma (10 ng/mL)/TNF- α -treated (30 ng/mL) WT and TTC7A-KO cells, 48 hours ($n = 3$). Refer to [Supplementary Figure 2C](#) for cleaved caspase 3 quantitation. RLU, relative light units.

confirmed loss of TTC7A expression ([Supplementary Figure 1](#)), and characterized cellular phenotypes associated with the loss of TTC7A ([Figures 1A–D](#), [Supplementary Figure 2](#)). Live-cell imaging showed that TTC7A-KO cells have abnormal morphology, including active membrane blebbing ([Figure 1A](#) and [Supplementary Video 1](#)). WT cells displayed normal spreading and colony formation, whereas TTC7A-KO cells were rounded with multiple membrane blebs and protrusions, a morphology that is associated with the early stages of apoptosis¹⁶ ([Figure 1A](#)).

We found that HAP1 TTC7A-KO cells have reduced cell viability ([Figure 1B](#)) and increased apoptosis using several complementary methods. Flow cytometry showed increased annexin V staining in TTC7A-KO cells, indicating that the cells were in the early stages of apoptosis ([Figure 1C](#) and [Supplementary Figure 2B](#)). Western blot analysis confirmed that TTC7A-KO cells have increased levels of baseline cleaved caspase 3 ([Figure 1D](#) and [Supplementary Figure 2C](#)). Additionally, we determined that TTC7A-KO cells have a greater susceptibility for caspase-dependent apoptosis after treatment with proinflammatory and proapoptotic stimuli (interferon gamma/tumor necrosis factor-

α [TNF- α]) ([Figure 1D](#)). Cumulatively, the data indicate that there is increased apoptosis in TTC7A-KO cells, mirroring a primary histopathologic feature found in patients with TTC7A-deficiency.^{1,2}

To examine cytoskeletal features underlying the abnormal morphology observed in TTC7A-KO cells we examined cellular actin. Actin staining showed abnormal cytoskeletal organization, with an abundance of filopodia-like processes in TTC7A-KO cells ([Supplementary Figure 3A](#)). Furthermore, when WT cells were treated with apoptotic stimuli (ie, proinflammatory cytokines interferon gamma/TNF- α), we observed disorganization of F-actin that resembled the untreated TTC7A-KO cells, suggesting that the baseline loss of TTC7A induces cellular changes consistent with induction and progression of apoptosis ([Supplementary Figure 3A](#)). We also observed that TTC7A-KO cells underwent apoptosis before substrate detachment ([Supplementary Figure 3B](#)), suggesting that cell death was not solely a result of anoikis (a form of apoptosis triggered by the loss of adhesion¹⁶). Taken together, we show that TTC7A-KO cells display phenotypes consistent with apoptosis.



Repurposing Drug Screen Identifies Hit Compounds That Reduce Apoptosis in TTC7A-KO Cells

Apoptosis is a pathologic feature of TTC7A loss observed both in vitro and clinically. We therefore designed a phenotypic drug screen to identify compounds that can reduce cellular apoptosis without inducing uncontrolled cell proliferation. We used a highly specific and sensitive luciferase-based caspase 3/7 activity assay (Caspase-Glo 3/7 [Promega, Madison, WI])¹⁷ for our primary screen. We developed the screen so that it could be multiplexed, where a single sample could provide readouts for both viability (using Calcein AM) and caspase 3/7 activity. Assessing for viability in parallel was advantageous because it increased the sensitivity and specificity of the screen by reducing false positives and ensuring that low caspase 3/7 readouts were not a result of compound toxicity and/or total cell annihilation. The Caspase-Glo 3/7 assay showed that TTC7A-KO cells consistently display elevated caspase 3/7 cleavage relative to WT cells, which resulted in a Z' -factor score of 0.54 (Figure 2A), a value that is suitable for discerning hits among thousands of compounds in a high-throughput screen.¹¹

A workflow schematic of our drug screen is provided in Figure 2B. With drug repurposing as the primary aim of our study, we selected 3 libraries (see Methods) containing FDA-approved drugs and other compounds with known biological targets. To ensure that hit identification was stringent, compounds that reduced caspase activity below 3 standard deviations of the positive control (ie, WT caspase 3/7 activity), providing a confidence limit of 99.73%, were selected as hits (see Figure 2C for a sample plate readout). We screened 3760 compounds and identified 16 compounds (henceforth referred to as *hits*), resulting in a 0.4% hit rate (Figure 2D and Figure 3). Nonsteroidal anti-inflammatory drugs (NSAIDs) and metabotropic glutamate receptor subtype 5 (mGluR5) antagonists were the most well represented drug classes among the hits.

All hits were confirmed via concentration-response curves in HAP1 TTC7A-KO cells (Supplementary Table 1). To ensure that hit compound efficacy was not an artefact

specific to TTC7A-KO cells, we further showed that our hit compounds could reduce caspase 3/7 activity in a HeLa cell line stably expressing TTC7A point mutations found in previously reported patients (p. E71K and A832T)¹ (Supplementary Table 1). Leflunomide was identified as the most efficacious compound based on its ability to inhibit caspase 3/7 activity (96% reduction) (Figure 2E) with an IC₅₀ concentration of 1.1 μ mol/L (Figure 2F).

Hit Compounds Rescue Concomitant Phenotypes Related to TTC7A Deficiency

From the 16 hit compounds identified in the screen, we selected a group of candidate drugs with pharmacologic class diversity and FDA-approved status for further validation. Our initial hits (Figure 3) were narrowed to 4 candidate drugs for orthogonal validation and included cyanocobalamin (vitamin B12), leflunomide (disease-modifying antirheumatic drug [DMARD]), tiaprofenic acid (NSAID), and fenbufen (NSAID). We also compared the performance of our candidate drugs with small molecule ROCK inhibitors (fasudil and Y27632) to determine whether aberrant TTC7A phenotypes might be driven by the constitutive activation of ROCK, as previously suggested.²

After treatment with the candidate drugs, the morphology of TTC7A-KO cells resembled that of WT cells with a reduction in membrane blebbing (Supplementary Figure 4). Cell colony size, a proxy for both cell adhesion and viability, was diminished in untreated TTC7A-KO cells; however, we observed the formation of larger-adherent colonies after cyanocobalamin, leflunomide, tiaprofenic acid, fasudil, and Y27632 drug treatments (Figure 2G and Supplementary Figure 4). In addition to reducing levels of apoptosis to that of the control, we found that candidate drug treatments improved the viability of TTC7A-KO cells over the course of 48 hours (Figure 2H), consistent with the observed increase in colony sizes. Importantly, because inhibition of apoptosis may result in excessive cell proliferation, we found that leflunomide improved viability to that of control levels, in contrast to the ROCK inhibitor fasudil, which increased viability above WT levels and induced excessive cell proliferation.

Figure 2. High-throughput drug screening identifies FDA-approved compounds that improve the apoptotic phenotype. (A) Modeling the high-throughput apoptosis-phenotype assay. Caspase-Glo 3/7 assay, $Z' = 0.54$, data are presented as the mean \pm standard deviation. Unpaired t test, **** $P < .0001$ ($n = 3$, 8 replicates). (B) Drug screen workflow. See Methods. (C) A sample of plate results from the Prestwick Chemical Library screen showing mean caspase 3/7 activity from drug-treated wells (green dots) and DMSO-treated control wells, WT (light blue dashes) and TTC7A-KO cells (dark blue dashes). Thiabendazole and tiaprofenic acid reduced caspase 3/7 activity below the hit threshold ($\mu_{WT} - 3\sigma$), $Z' = 0.56$. (D) Drug screen summary, 0.4% hit rate. Hit compounds represent the 10 drug classification families shown. (E) Comparison of hit compound inhibition of apoptosis in TTC7A-KO cells. Black borders represent FDA-approved drugs and bar colors correspond to Figure 2D. (F) Concentration-response curve for leflunomide inhibition of caspase 3/7 activity in HAP1 TTC7A-KO cells; IC₅₀ = 1.1 μ mol/L ($n = 3$). (G) Colony size formation in WT, TTC7A-KO, and drug-treated TTC7A-KO cells. Plotted values represent individual cell colonies; error bars presented as mean \pm standard deviation. Statistical significance was relative to the KO/DMSO control. One-way ANOVA with post hoc test (Dunnett), **** $P < .0001$, *** $P < .001$, ** $P < .01$ ($n = 3$, 6 replicates per condition). (H) Viability assay. Statistical significance relative to KO/DMSO (blue). WT, * $P < .05$; KO/LEF, ** $P < .01$; KO/TIA, **** $P < .0001$; KO/FEN, *** $P < .001$; KO/FAS, **** $P < .0001$; 2-way ANOVA with post hoc test (Dunnett) ($n = 3$, 4 replicates per condition). CYANO, cyanocobalamin; FAS, fasudil; FEN, fenbufen; LEF, leflunomide; M, mol/L; RLU, relative light units; TIA, tiaprofenic acid.

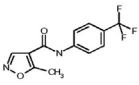
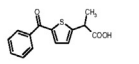
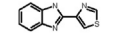
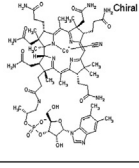
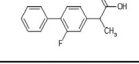
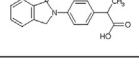
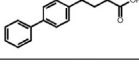
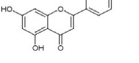
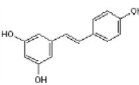
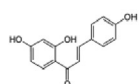
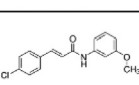
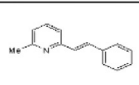
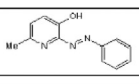
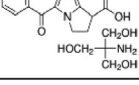
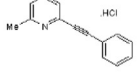
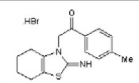
Compound Name	Structure	Formula Structure	Molecular Weight (g/mol)	IC 50 (μM)	Decrease in caspase 3/7 activity	Compound description
Leflunomide		C ₁₂ H ₉ F ₃ N ₂ O ₂	270.2	1.1	96%	Disease Modifying Anti-Rheumatic Drug (DMARD) - Pyrimidine synthesis inhibitor
Tiaprofenic acid		C ₁₄ H ₁₂ O ₃ S	260.3	2.5	87%	NSAID, arthritic pain
Tiabendazole		C ₁₀ H ₇ N ₃ S	201.3	11	60%	Fungicide and anthelmintic
Cyanocobalamin		C ₆₃ H ₈₈ CoN ₁₄ O ₁₄ P	1355	11	64%	Vitamin B12
Flurbiprofen		C ₁₅ H ₁₃ FO ₂	244.2	39	31%	NSAID, arthritic pain
Indoprofen		C ₁₇ H ₁₅ NO ₃	281.3	6.1	73%	NSAID, withdrawn due to carcinogenicity
Fenbufen		C ₁₆ H ₁₄ O ₃	254.3	30	56%	NSAID, osteoarthritis, ankylosing spondylitis, and tendinitis
Acacetin		C ₁₆ H ₁₂ O ₅	284.3	N/A	47%	Flavone, anticonvulsant and plant metabolite
Resveratrol		C ₁₄ H ₁₂ O ₃	228.3	4.9	45%	Stilbenoid, anti-inflammatory, polyphenolic phytoalexin
Isoliquiritigenin		C ₁₅ H ₁₂ O ₄	256.3	9.7	89%	Soluble guanylyl cyclase activator
SB-366791		C ₁₆ H ₁₄ NO ₂ Cl	287.7	7.6	58%	Vanilloid antagonist
SIB 1893		C ₁₄ H ₁₃ N	195.3	9.1	58%	Selective antagonist of metabotropic glutamate receptor (mGlu5R)
SIB 1757		C ₁₂ H ₁₁ NO	213.2	18	50%	Selective antagonist of mGlu5R
Ketorolac tris salt		C ₁₅ H ₁₂ NO ₃ ·C ₄ H ₁₂ NO ₃	376.4	156	48%	NSAID
MPEP hydrochloride		C ₁₄ H ₁₁ N.HCl	229.7	6.3	33%	Selective antagonist of mGlu5R
Pifithrin- α hydrobromide		C ₁₆ H ₁₈ N ₂ O ₂ ·HBr	367.3	8.3	31%	p53 inhibitor

Figure 3. Summary of Hits Able to Reduce Caspase 3/7 Activity in TTC7A-KO Cells. Shaded boxes indicate FDA-approved drugs. Compound structures, formulas, and molecular weights were provided by Prestwick, LOPAC, and Tocriscreen, and compound descriptions were obtained from PubChem.²⁷

Leflunomide Rescues Abnormal Intestinal Features in *ttc7a*^{-/-} Zebrafish

To date, a major obstacle in TTC7A research is the lack of an appropriate disease model that recapitulates the intestinal abnormalities observed in patients with TTC7A deficiency. For example, *Ttc7a*-mutant mice display a prominent flaky skin phenotype but do not manifest the atretic and inflamed intestinal phenotypes seen in patients.¹⁸ We therefore sought to develop an animal model able to phenocopy the intestinal abnormalities seen in humans. Using CRISPR-Cas9 genome editing, we developed and validated a *ttc7a* zebrafish line (*ttc7a*^{-/-}) with an 11-base-pair deletion in exon 14 predicted to result in a frameshift mutation causing an early stop codon (p.T548LfsX41) (Supplementary Figure 5 and Supplementary Table 2).

The *ttc7a*^{-/-} zebrafish (*ttc7a*-mutant) have normal survival but display a range of abnormal intestinal phenotypes (Figure 4). Histopathologic zebrafish sections were taken along the sagittal plane to assess a continuous stretch of the intestinal tract, including the widest and most anterior intestine (the intestinal bulb [IB]) to the anal pore (Figure 4A). Sections were assessed for an open IB, villus structure, a discernable epithelial monolayer, intestinal epithelial cell integrity, and the presence of mature goblet cells with large secretory vesicles. Histologic examination showed that *ttc7a*^{-/-} zebrafish had a combination of the following intestinal defects: stratification and crowding of intestinal epithelial cells, blunted villi, breaches in the intestinal mucosal layer, signs of apoptosis, and atresia along the intestinal tract (Figure 4A). The intestinal defects observed from zebrafish histology were consistent with patient histopathologic findings,^{1,2,4} suggesting that *ttc7a*-mutant fish appropriately model the intestinal atresia and loss of intestinal epithelial cell integrity observed in TTC7A patients.

Intestinal atresia is a distinctive phenotype among patients with TTC7A deficiency. Similarly, intestinal narrowing was the most striking abnormality in *ttc7a*-mutant fish (Figure 4B and Supplementary Figure 6). There was a greater than 50% incidence of intestinal narrowing in the *ttc7a*-mutant fish population, whereas this phenotype was minimal (<5%) in control fish. We showed that leflunomide treatment of *ttc7a*-mutant fish resulted in a reduced incidence of intestinal narrowing, suggesting that the drug ameliorated intestinal atresia formation (Figure 3B).

The *ttc7a*^{-/-} fish showed additional histologic improvement, including increases in the size of intestinal luminal spaces and discernible villi and goblet cell morphology after treatment with tiaprofenic acid, leflunomide, or cyanocobalamin (Figure 4C). Intact monolayers with normal columnar intestinal cell architecture and fewer apoptotic cells were observed in leflunomide-treated *ttc7a*^{-/-} fish (Figure 4D and Supplementary Figure 7A). Previous studies suggested that the chaperone drug 4-PBA (Ucyclyd Pharma), and ROCK-inhibitors (fasudil and Y27632) may be effective in improving defects related to TTC7A deficiency.^{2,9} Our data suggest that 4-PBA treatment improves intestinal defects seen in *ttc7a*^{-/-} fish, in contrast to the ROCK inhibitors, which did not result in any histologic improvements (Supplementary Figure 8).

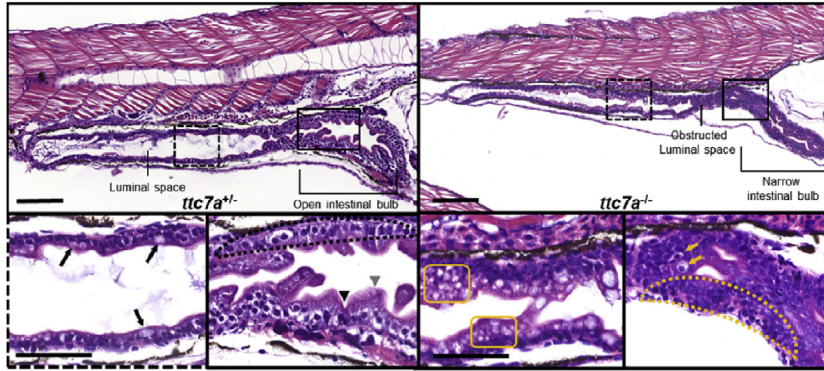
The histopathologic findings were further validated by real-time in vivo imaging of intestinal peristalsis, which showed differences in gut architecture and contractile motility (Figure 4E and Supplementary Video 2). Normal motility is integral to intestinal health, and loss of intestinal contractility is correlated with increased IBD severity.¹⁹ Live-labeling of the intestinal lumen was achieved by treating the fish with a water-soluble nonfluorescent stain, 2',7'-dichlorodihydrofluorescein diacetate (DCFH-DA), that becomes oxidized to a fluorescent compound once ingested by the fish.¹³ Still frames from peristalsis imaging are shown in Figure 3E, and corresponding footage can be found in Supplementary Video 2. Normal intestinal architecture, including the presence of distinct villi, can be appreciated with light transmission (differential interference contrast) imaging, and delineation of a distinct luminal space can be seen by epifluorescence imaging. Control heterozygous fish, *ttc7a*^{+/-}, consistently displayed coordinated peristaltic contractions and larger intestinal luminal spaces with discernable villi in the IB (Figure 4E and F and Supplementary Video 2). Peristalsis assays showed that *ttc7a*^{-/-} fish have narrow regions in the anterior IB, resulting in bottlenecked contractions, severely narrow luminal spaces with absent peristalsis, and masses obstructing the IB, resulting in uncoordinated gut motility (Figure 4E and F). In sum, we show that *ttc7a*-mutant fish have intestinal atresia resembling that of patients with TTC7A deficiency^{1,2,4} with severe atretic phenotypes.

Candidate drug treatment of *ttc7a*-mutant fish showed that leflunomide reduced the proportion of mutant fish with motility defects, rescued the atresia phenotype, and increased intestinal luminal volumes (Figure 4G and Supplementary Figure 7B). Leflunomide treatment also resulted in the largest improvement in motility observed in *ttc7a*^{-/-} fish (Figure 4G). Except for fenbufen, all candidate drugs increased intestinal luminal volume. (Supplementary Figure 7B). Taken together, we show that leflunomide is effective in improving gut motility and intestinal epithelium integrity and preventing intestinal atresia in *ttc7a*^{-/-} fish.

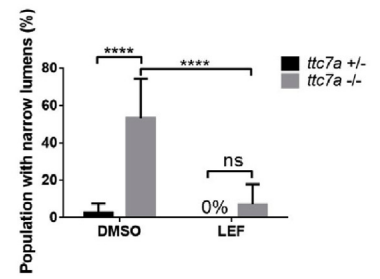
The Role of AKT in TTC7A Deficiency

AKT is a crucial survival kinase, and its activation (via phosphorylation) prevents apoptosis, promotes proliferation, increases protein expression, and regulates cell metabolism.⁷ Given that reduced viability and increased apoptosis were conspicuous TTC7A-deficiency phenotypes, we sought to determine whether TTC7A dysfunction might alter AKT activation. We observed that patients with TTC7A deficiency had loss of phosphorylated-AKT (p-AKT) in the intestinal epithelium, whereas changes in total AKT levels were less striking, suggesting that AKT activation (ie, p-AKT levels) may be tied to the pathobiology of TTC7A deficiency (Figure 5A and B). We examined AKT signaling using the HAP1 cell line. As shown in Figure 5C, WT cells lack cleaved caspase 3 and have measurable levels of both p-AKT and X-linked inhibitor of apoptosis (XIAP), in contrast to TTC7A-KO cells, which exhibit the presence of cleaved caspase 3 and reduction in p-AKT and XIAP levels. Treatment

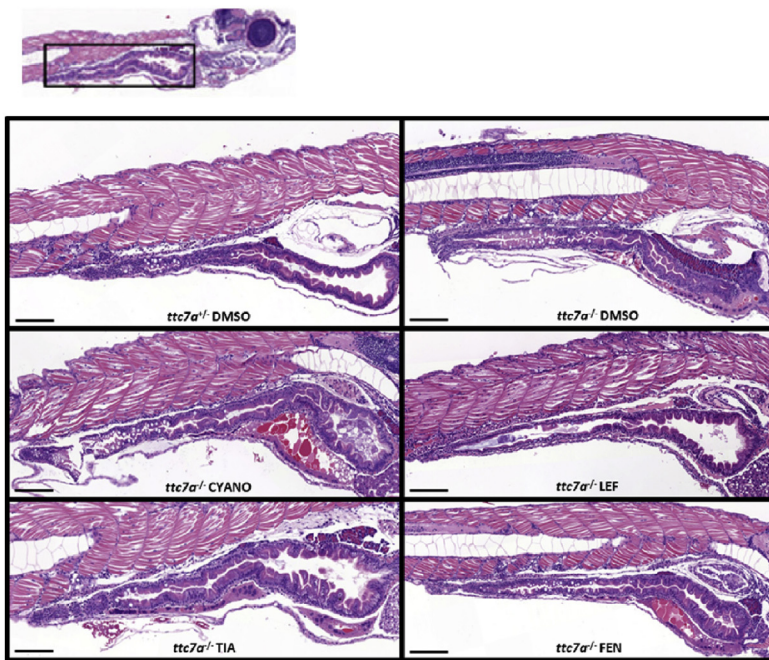
A



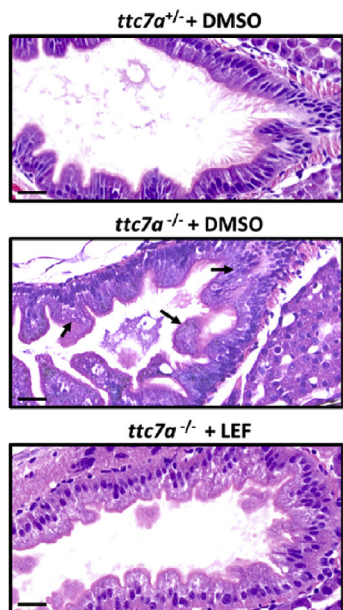
B



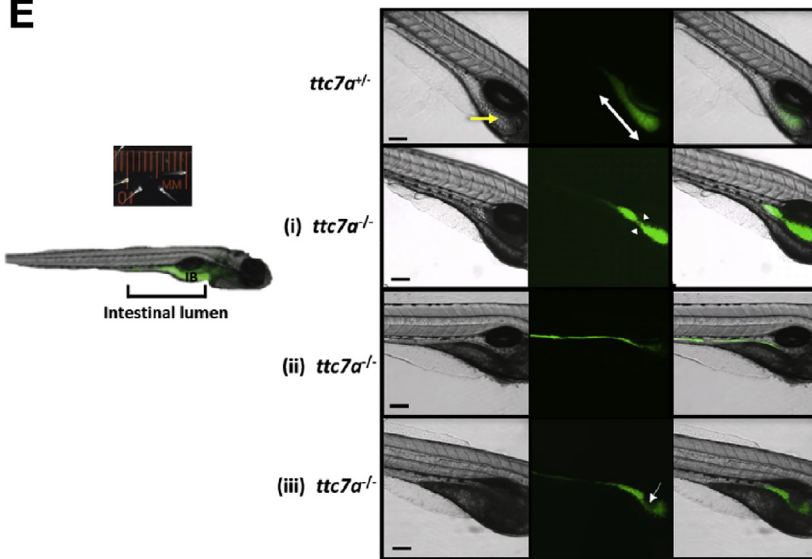
C



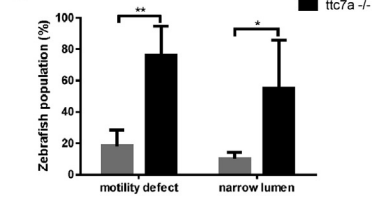
D



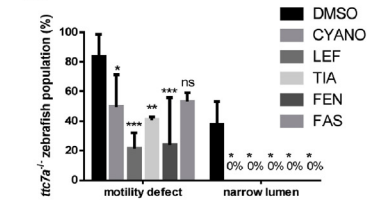
E



F



G



with a phosphatidylinositol 3-kinase (PI3K) inhibitor (LY294002) blocks the formation of PI(3,4,5)P₃ required for AKT activation and triggers caspase 3 cleavage.⁷ WT cells treated with PI3K inhibitor show a similar immunoblot pattern to TTC7A-KO cells treated with DMSO, suggesting that the apoptotic phenotype observed in TTC7A deficiency may be mediated by AKT (Figure 5C). Importantly, TTC7A-KO cells treated with leflunomide resulted in an increase in p-AKT (threonine 308) and XIAP and a reduction in cleaved caspase 3 levels (Figure 5D). These data suggest that leflunomide may improve cell viability and reduce apoptosis by altering AKT activation. Furthermore, treatment with the PI3K inhibitor resulted in undetectable AKT phosphorylation at both threonine 308 and serine 473 sites in WT and leflunomide-treated TTC7A-KO cells, suggesting that leflunomide is acting upstream of PI3K (Supplementary Figure 9).

The inhibition of pyrimidine synthesis via dihydroorotate dehydrogenase (DHODH) is the putative target of leflunomide.¹⁰ Immunoblot analysis using vidofludimus, another DHODH inhibitor, did not increase p-AKT or reduce cleaved caspase 3, suggesting that leflunomide increases p-AKT via an uncharacterized mechanism (Supplementary Figure 10). Treatment of TTC7A-KO cells with leflunomide results in a shift from an apoptotic to a survival phenotype; however, leflunomide's mechanism for altering p-AKT, XIAP, and cleaved caspase 3 remains to be elucidated.

We also performed whole-mount zebrafish staining that confirmed the loss of p-AKT (Figure 5E). Leflunomide was able to increase p-AKT levels in the gastrointestinal tract of *ttc7a*^{-/-} fish, thus, providing in vivo drug validation in the

zebrafish model (Figure 5E). These data point to AKT as a possible therapeutic target for restoring intestinal health in TTC7A deficiency.

Leflunomide Treatment Enhances Survival and Function of TTC7A Deficiency Patient-Derived Colonoids

To further validate the effect of leflunomide, we tested the drug's efficacy in colonoids derived from patients with TTC7A deficiency. Biopsy samples were obtained from a 6-month-old female with confirmed biallelic *TTC7A* mutations (*TTC7A*^{mut}), c.211 G>A (p.E71K) and c.911delT (p.L304R) (Figure 6A). *TTC7A* immunofluorescence staining of a colonic tissue sample showed that the sample from the patient with *TTC7A*^{mut} had loss of *TTC7A* staining compared with the healthy and IBD control samples (Supplementary Figure 11A). Histologic sections obtained from *TTC7A*^{mut} patient intestinal biopsy specimens also showed features consistent with *TTC7A* deficiency, including villous blunting in the duodenum and crypt apoptosis and eosinophilic inflammation in the colon (Supplementary Figure 11B).

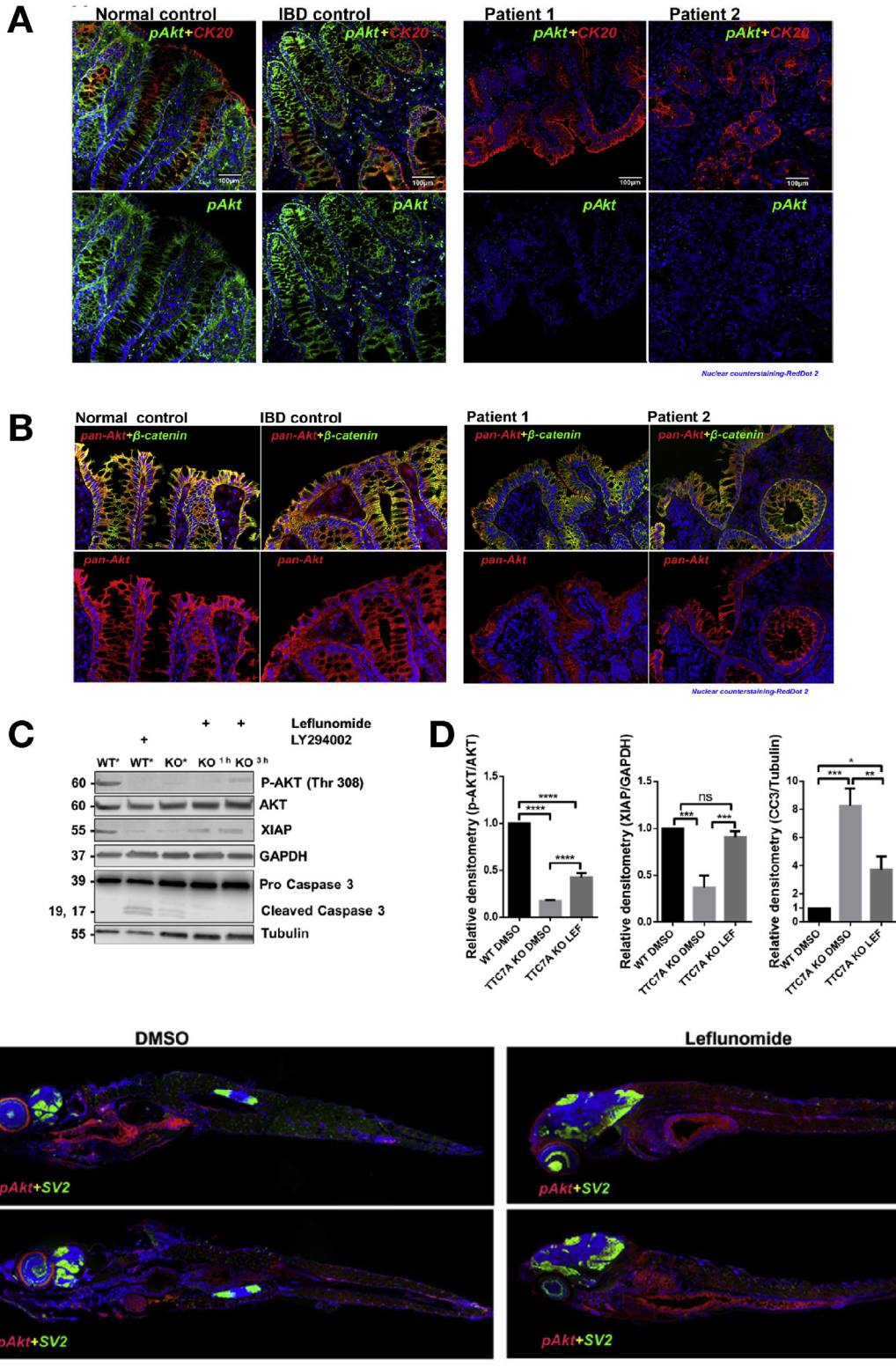
Previous studies have shown that ROCK inhibition is able to improve survival of *TTC7A*-deficient organoids.² Colonoids derived from both a healthy individual (*TTC7A*^{+/+}) and our patient with *TTC7A*^{mut} were generated from endoscopic biopsies and treated with a ROCK inhibitor (5 μmol/L Y27632) and/or leflunomide. Compared with control *TTC7A*^{+/+} colonoids, a higher percentage of *TTC7A*^{mut} colonoids died in the absence of ROCK inhibitor treatment (Figures 6B and C). Treatment of *TTC7A*^{mut}

Figure 4. Leflunomide rescues abnormal intestinal features in *ttc7a*^{-/-} zebrafish. (A) Histology from *ttc7a*^{-/-} zebrafish (7 dpf) shows pathologic intestinal phenotypes. Control (*ttc7a*^{+/+}) zebrafish display open luminal spaces with discernible villi projections (gray arrowhead), clefts (black arrowhead), monolayer epithelium (dotted-outlined area), and mature goblet cells with large vesicles (black arrows). The *ttc7a*^{-/-} zebrafish display narrowing of the intestinal bulb, stratified epithelium (yellow dotted-outlined area), signs of apoptosis (yellow arrows), and goblet cells with numerous small vesicles (yellow boxes). Original objective magnification, ×10 and ×40 for insets (scale bar, 100 μm; inset scale bar, 50 μm) (*ttc7a*^{+/+}: N = 14, *ttc7a*^{-/-}: N = 11). (B) Incidence of the narrow gut phenotype in DMSO- and LEF-treated fish. One-way ANOVA with post hoc test (Fisher least significant difference), *****P* < .0001; (*ttc7a*^{+/+}: DMSO, N = 49; LEF, N = 12; *ttc7a*^{-/-}: DMSO, N = 36; LEF, N = 26). (C) Intestinal histology from treated (see Methods) *ttc7a*^{-/-} zebrafish. Leflunomide, cyanocobalamin, and tiaprofenic acid suppressed the narrow-gut phenotype with minimal enterocyte crowding. Original objective magnification, ×10 (scale bar, 100 μm) (*ttc7a*^{+/+}: DMSO, N = 49; *ttc7a*^{-/-}: DMSO, N = 36; CYANO, N = 10; LEF, N = 26; TIA, N = 13; FEN, N = 13). (D) Assessment of apoptosis. DMSO or leflunomide treatment. *ttc7a*^{-/-} zebrafish display fragmented, condensed, or engulfed nuclei in the epithelium (arrows). Leflunomide treatment resulted in diminished signs of apoptosis, reduced intestinal epithelial cell crowding, and overall improved epithelium architecture in *ttc7a*^{-/-} zebrafish. Refer to Supplementary Figure 7A for the quantitation of apoptotic cells/sample. Objective magnification, ×70 (scale bar, 20 μm) (n = 6 per group, across 3 experimental clutches). (E) Staining of the intestinal lumen in control (*ttc7a*^{+/+}) and *ttc7a*-mutant (*ttc7a*^{-/-}) zebrafish. Images are from peristalsis assays (Supplementary Video 2): intestinal lumen marked by green fluorescent stain, 2',7'-dichlorodihydrofluorescein diacetate (DCFH-DA). The *ttc7a*^{+/+} fish have discernible villi (yellow arrow) and large continuous intestinal bulbs (double-headed white arrow). Representative *ttc7a*^{-/-} intestinal phenotypes (i) atresia point (white arrow heads) (ii) narrow intestinal lumen and (iii) obstruction interrupting the intestinal bulb (white arrow). Objective magnification ×4 (scale bar, 100 μm). (F) Incidence of *ttc7a*-mutant phenotypes. The *ttc7a*^{-/-} fish have significantly larger populations with motility and narrow lumen pathologic phenotypes. Data are presented as the mean ± standard deviation; 1-way ANOVA with post hoc test (Fisher least significant difference), ***P* < .0054, **P* < .0196 (N = 50 total for each group, across 3 experimental clutches). (G) Phenotype summary from drug-treated fish. The *ttc7a*^{-/-} fish with aberrant motility and narrow lumen phenotypes were significantly reduced with cyanocobalamin, leflunomide, tiaprofenic acid, and fenbufen treatment (3–7 dpf). Data are presented as the mean ± standard deviation. Statistical significance was relative to *ttc7a*^{-/-} DMSO control and determined by 2-way ANOVA with post hoc test (Dunnett) **P* < .05, ***P* < .01, ****P* < .001 (DMSO: N = 18; CYANO: N = 21; LEF: N = 21; TIA: N = 17; FEN: N = 18; FAS: N = 13 for each group across 3 experimental clutches). CYANO, cyanocobalamin; FAS, fasudil; FEN, fenbufen; LEF, leflunomide; M, mol/L; ns, not significant; RLU, relative light units; TIA, tiaprofenic acid.

colonoids with leflunomide (with and without ROCK inhibitor) promoted colonoid survival in a dose-dependent manner.

Apicobasal polarity is essential to intestinal epithelial cell function, and previous studies have suggested aberrant

cell polarity in TTC7A-deficient epithelial cells.² Intact TTC7A^{+/+} colonoids showed well-demarcated polarization of apical and basolateral membranes delineated by villin and cytokeratin 20 (CK20) staining, respectively (Figure 6D). Without ROCK-inhibitor treatment, epithelial



cells were polarized in the correct orientation in TTC7A^{mut} colonoids, yet they showed other defects, including disorganized cytoskeletal staining, the presence of abnormal cytoplasmic inclusions and the presence of multiple lumens. In conjunction with previous reports² in which treatment with a ROCK inhibitor restored epithelial structure and polarity in TTC7A-deficient colonoids, TTC7A^{mut} colonoids treated with a ROCK inhibitor partially corrected polarity defects, as assessed by the number of colonoids with multiple lumens (Figure 6D). Similar to the ROCK-inhibitor treatment, leflunomide (10 μ mol/L) also partially rescued cytoskeletal and polarity defects in TTC7A^{mut} colonoids.

Transepithelial fluid and electrolyte homeostasis are essential functions of intestinal epithelial cells. Therefore, to assess whether leflunomide can restore epithelial function in TTC7A deficiency, we measured agonist-stimulated fluid secretion in intact colonoids. Fluid secretion was stimulated by addition of the adenosine 3'5'-cyclic monophosphate-elevating agonist forskolin, which activates cystic fibrosis transmembrane conductance regulator (CFTR)-mediated anion and fluid transport into the lumen of the colonoid. Fluid secretion can then be measured by the extent of colonoid swelling.¹⁵ TTC7A^{mut} colonoids have impaired agonist-stimulated fluid secretion compared with control TTC7A^{+/+} colonoids (Supplementary Figure 11C and D). However, in TTC7A^{mut} colonoids, leflunomide was able to restore the ability of the epithelium to secrete fluid, suggesting recovery of epithelial transport function (Figures 6E and F). These data from TTC7A-deficient patient cells suggest that leflunomide treatment can improve intestinal epithelial survival, structure, and ion transport function in humans.

Discussion

TTC7A deficiency is a rare and often fatal disease that disrupts intestinal epithelial homeostasis and the immune system.^{1,2} Challenged by the unmet need for therapies and reports that immune reconstitution via hematopoietic stem cell transplant do not improve the intestinal disease,⁵ our goal was to identify candidate drugs that improve intestinal abnormalities. Given that apoptosis is a key clinical and experimental feature of TTC7A deficiency, we performed a phenotypic high-throughput drug screen to identify

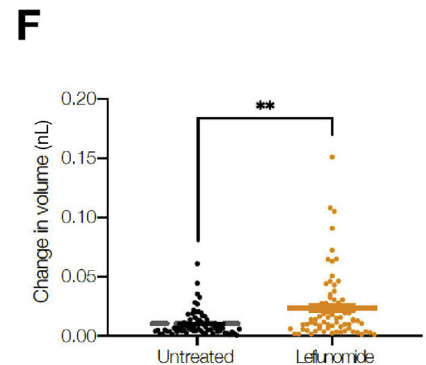
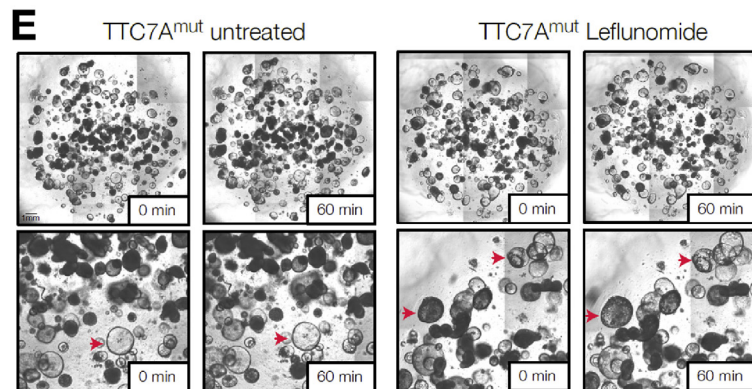
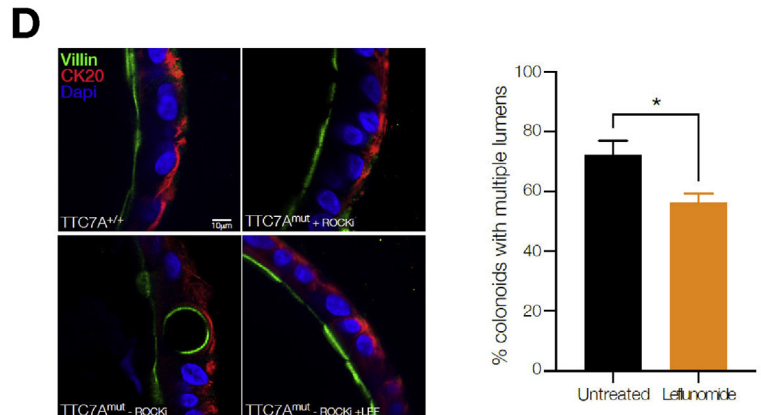
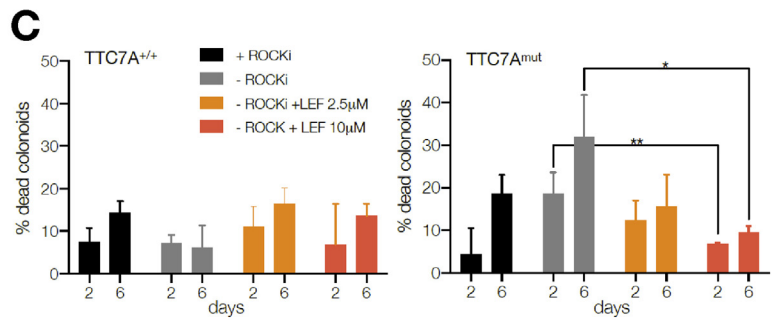
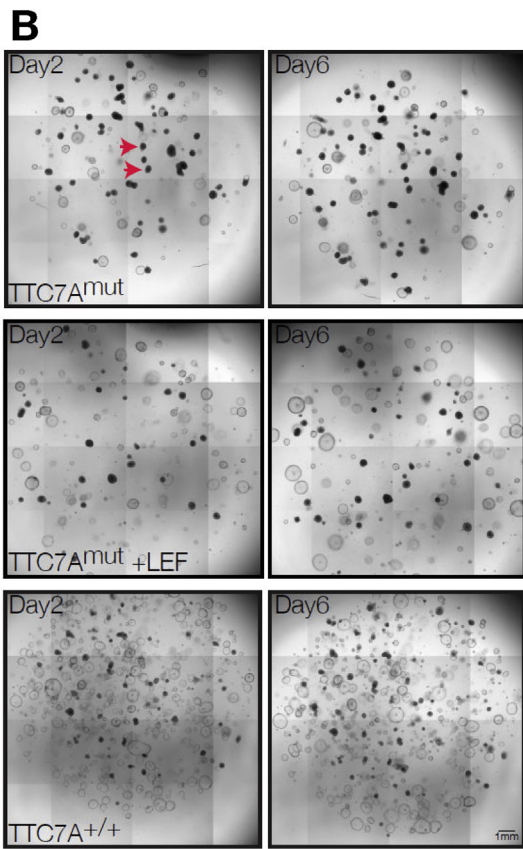
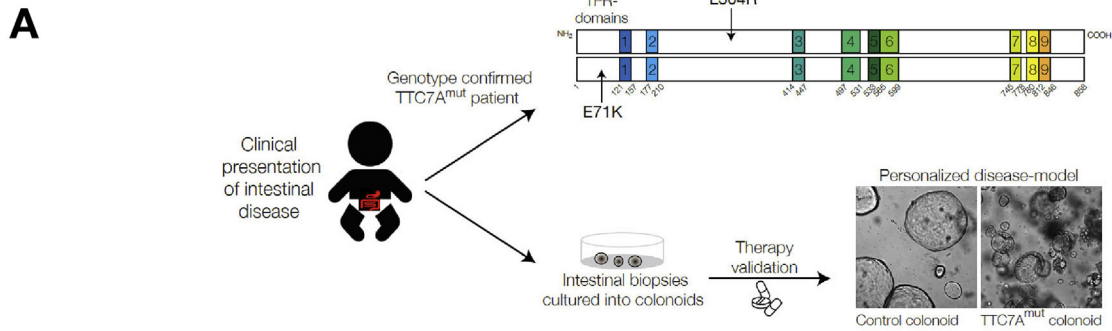
compounds that could reduce the increased apoptosis seen in TTC7A deficiency. We selected candidate drugs having class diversity, known safety profiles, and repurposing potential and tested their efficacy in various disease models. Based on our experimental data, safety profiles, FDA-approved status, and its prior use for inflammatory conditions such as juvenile rheumatoid arthritis,²⁰ leflunomide was selected as our lead candidate therapeutic. Leflunomide's known mechanism of action is through inhibition of DHODH, an enzyme responsible for the de novo synthesis of pyrimidines important in T-cell activation.¹⁰ However, vidofludimus, a selective DHODH inhibitor,²¹ did not increase p-AKT or inhibit cleaved caspase 3 in TTC7A-KO cells, indicating an alternative mechanism of action in rescuing TTC7A-deficient cells. We showed that leflunomide is involved in regulating AKT, providing a potential mechanism for the increase in cell viability and reduction in apoptosis. These findings corroborate the research from Leger et al²² showing that low-dose leflunomide (10 μ mol/L) activates PI3K/AKT signaling in HEL and K562 leukemia cells.²² We propose that loss of AKT activation in TTC7A deficiency results in a greater susceptibility for caspase 3 cleavage, thereby altering cellular fitness and disrupting epithelial homeostasis (Figure 7).

A phase 1 clinical study and uncontrolled pilot study suggested that leflunomide may be a safe treatment option for Crohn's disease, although not commonly used.²³ Besides leflunomide, there were other potential candidate drugs. Although tiaprofenic acid was able to rescue many TTC7A-related phenotypes, its repurposing should be approached with caution because it is typically not prescribed for children, and NSAIDs are associated with gastric bleeding.²⁴ Cyanocobalamin, the synthetic form of vitamin B12, was less effective in rescuing the apoptotic phenotype compared with leflunomide; however, its relatively safe clinical profile makes it an appealing therapeutic to consider. Additionally, there is some limited evidence that high-dose vitamin B12 may be beneficial in patients with IBD.²⁵ Interestingly, 3 hits (non-FDA-approved drugs) were antagonists of mGluR5, a type of G-protein-coupled receptor linked to the inositol trisphosphate/diacylglycerol pathway. Previous research shows mGluR5 antagonists to be important in the gastrointestinal tract by improving epithelial barrier function.²⁶ The drug screen herein

Figure 5. p-AKT is reduced in TTC7A deficiency. (A) Histopathology analysis of p-AKT in human colon tissue. Costaining of CK20, a marker for the intestinal epithelium, and p-AKT is present in the normal and IBD control samples, whereas p-AKT is diminished in patients with TTC7A-deficiency. Patient 1 is the colonoid donor, and patient 2 is unpublished with confirmed biallelic mutations. RedDot 2 nuclear counterstain (blue). Sections were originally magnified at $\times 20$ objective. (B) Histopathology analysis of pan-AKT (total AKT) in human colon tissue. Biopsy samples are the same as those described in Figure 5A. Pan-AKT is present in all samples, albeit with reduced intensity in the TTC7A-deficiency patient samples. Sections were originally magnified at $\times 20$ objective. (C) Immunoblot for p-AKT, XIAP, and cleaved caspase 3 in WT and TTC7A-KO cells. After 3 hours, leflunomide treatment in TTC7A-KO cells, p-AKT, and XIAP protein levels are detectable, whereas cleaved caspase 3 is diminished. Asterisk indicates DMSO (n = 3). (D) Densitometric analysis of p-AKT, XIAP, and cleaved caspase 3 from WT and TTC7A-KO cells. One-way ANOVA with post hoc test (Tukey); * $P < .05$, ** $P < .01$, *** $P < .001$, **** $P < .0001$ (n = 3). (E) The *ttc7a*^{+/-} and *ttc7a*^{-/-} whole-mount zebrafish staining with p-AKT (red), synaptic vesicle protein 2 (SV2) (green), and RedDot 2 nuclear counterstain (blue). SV2 staining, indicating neuromuscular junctions, is absent from the intestinal epithelial monolayer and aids in differentiating epithelial cells from other nearby cell types. In the DMSO-treated panel, p-AKT staining (Ser473) in *ttc7a*^{+/-} fish is evident along the gastrointestinal tract but absent in *ttc7a*^{-/-} fish. Leflunomide treatment (3-7 dpf) restores p-AKT staining in the intestinal epithelium of *ttc7a*^{-/-} fish. Fish were originally magnified at $\times 5$ objective (n = 4).

identified a diverse range of biologically active compounds and illuminated potential pathways implicated in TTC7A deficiency.

We showed that *ttc7a*-mutant zebrafish have intestinal atresia, loss of villi, discordant intestinal epithelial cell integrity, and poor gut motility. The zebrafish model



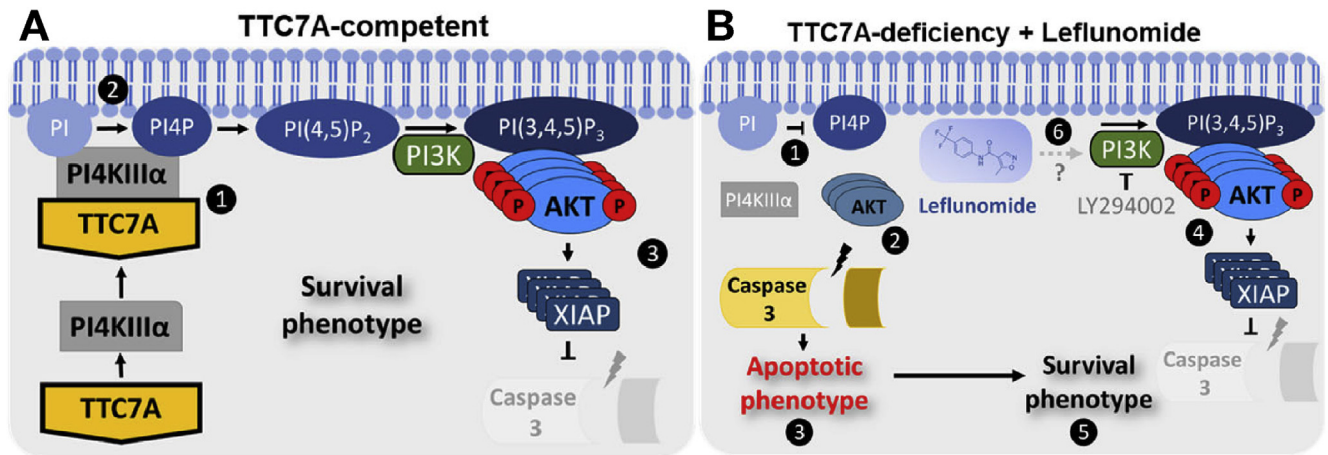


Figure 7. Model of leflunomide’s mechanism of action in TTC7A deficiency. (A) TTC7A-competent. (1) TTC7A binds and recruits PI4KIII α to the plasma membrane. (2) PI4KIII α phosphorylates PI lipids to create PI4P, a precursor to PI (4,5)P₂/PI(3,4,5)P₃. (3) PI3K phosphorylates PI (4,5)P₂, required for AKT phosphorylation. p-AKT activates multiple downstream substrates that promote cell survival. For example, XIAP polyubiquitylates pro-caspases 3,7, and 9 for proteasomal degradation, thereby reducing the susceptibility for caspase-dependent cell death. (B) TTC7A deficiency plus leflunomide. (1) PI4KIII α trafficking to (or kinase activity at) the plasma membrane is compromised in TTC7A deficiency, resulting in reduced PI4P. (2) Reduced p-AKT provides a rationale for increases in apoptosis. (3) caspase-dependent apoptosis is frequently associated with TTC7A deficiency. (4) Leflunomide treatment increases p-AKT and XIAP levels. (5) The apoptotic phenotype is ameliorated when TTC7A-deficient HAP1 cells are treated with leflunomide, suggesting a shift toward a survival phenotype. (6) It has yet to be established how leflunomide mediates p-AKT activation; however, PI3K inhibition with LY294002 hinders leflunomide’s effect on AKT, XIAP, and caspase 3 cleavage.

recapitulates the intestinal phenotypes seen in patients, and, to our knowledge, establishes the only animal disease model system for TTC7A deficiency. Consistent with the mechanism of our model, Thakur and colleagues⁹ developed a zebrafish model (*cdipt^{hi559}*) lacking PI synthesis and, interestingly, also observed an intestinal atresia phenotype, thus providing a precedent for linking PI deficiency with IBD and intestinal narrowing. Taken together, these findings further suggest that PI regulation could be an important target for improving intestinal health.

The GI tracts of zebrafish and humans have homologous structures, functions, tissues, and cell types, and their transparency during the larval stage makes for an advantageous model for intestinal research.⁹ However, fundamental differences in zebrafish and humans (eg, microbiome, environmental) could possibly contribute to the discrepancies we see in disease severity and overall survival. Ultimately, differences in the microbiome, embryonic development, and drug dosing increase the complexity in translating these findings to patients. A

BASIC AND TRANSLATIONAL AT

Figure 6. Leflunomide treatment enhances survival and function of TTC7A-deficiency patient colonoids. (A) A personalized medicine approach to evaluate drug efficacy in human TTC7A deficiency using patient-derived colonoids. Endoscopic biopsy samples were obtained from healthy control individuals and patients with TTC7A deficiency (E71K and L304R compound heterozygous, TTC7A^{mut}) and cultured into colonoids, which were then tested with leflunomide. (B) Leflunomide improves the survival of human colonoids derived from patients with TTC7A-deficiency (TTC7A^{mut}). Example images of control (TTC7A^{+/+}) and TTC7A-deficient (TTC7A^{mut}) colonoids with and without leflunomide (10 μ mol/L) treatment at 2 and 6 days and grown in the absence of ROCK inhibitor (Y27632). Red arrows indicate examples of dead colonoids. (C) Summary graph showing the percentage of dead TTC7A^{mut} colonoids with and without leflunomide treatment. TTC7A^{mut} and TTC7A^{+/+} colonoids were cultured with and without ROCK inhibitor (Y27632) or with leflunomide, and viability was assessed at days 2 and 6. TTC7A^{mut} colonoids grown without ROCK inhibitor have significantly increased death, which is reversed after leflunomide treatment. One-way ANOVA with post hoc test (Tukey-Kramer); **P* < .05. ***P* < .01. (D) Immunofluorescence staining of TTC7A^{+/+} and TTC7A^{mut} colonoids with villin (green) marking the apical brush border and CK20 (red) marking basal epithelial structure and DAPI (blue, nuclei). TTC7A^{+/+} colonoids show normal polarity with defined basal CK20 staining. TTC7A^{mut} colonoids treated with ROCK inhibitor show grossly normal staining with mild cytological atypia. TTC7A^{mut} colonoids without ROCK inhibitor show normal sidedness but abnormal polarity with cytological atypia and basal structural abnormalities, which is improved in leflunomide-treated colonoids. Quantification of abnormal polarity, as assessed by the presence of multiple lumens in colonoids. Percentage of colonoids with multiple lumens in TTC7A-deficient colonoids with and without leflunomide (10 μ mol/L). Healthy control colonoids did not have multiple lumens (data not shown). Two tailed *t* test, **P* < .05. (E, F) TTC7A-deficient colonoids (TTC7A^{mut}) have a reduced swelling response to forskolin stimulation. Example images showing reduced swelling in TTC7A^{mut} compared with TTC7A^{mut} treated with leflunomide (10 μ mol/L). The inset panel shows magnified images, with red arrows indicating example colonoids before and after swelling. Summary data show significantly increased swelling in leflunomide (10 μ mol/L)-treated TTC7A^{mut} colonoids. Two-tailed *t* test, ***P* < .01.

thorough characterization of intestinal apoptosis in *ttc7a*-mutant fish is additionally required and may help elucidate the extent of morbidity that is driven by cell death. Also, given that the fish were treated with leflunomide from 3 to 7 dpf, and that the gut is fully formed by 5 dpf, it remains to be elucidated whether leflunomide prevents or reverses the intestinal pathologies. In the future, the development of transgenic *ttc7a*^{-/-} reporters that aid in visualizing intestinal infiltrate may allow for more thorough assessment of histopathologic features in *ttc7a*-deficient fish.

Despite leflunomide's merits of approved status and previous use in pediatrics, several limitations exist. Clinically, existing data pertaining to leflunomide's pharmacokinetics, IC₅₀ values, and mechanism of action are specific to its use in rheumatoid arthritis and inhibition of pyrimidine synthesis via DHODH. In our study, leflunomide's precise mechanism of action remains to be elucidated, and previously reported IC₅₀ values differ because they are for the inhibition of DHODH rather than caspase activity. Identifying leflunomide's primary cellular target may therefore be critical to fully understanding how TTC7A functions in intestinal cells. Our study identified leflunomide's IC₅₀ for the inhibition of caspase 3/7 activity *in vitro*, but potency remains to be established for the *in vivo* situation, with alterations likely due to drug pharmacokinetics. Current juvenile rheumatoid arthritis dosing for leflunomide may differ for patients with TTC7A-deficiency who are likely to be very young (<6 years). Therefore, establishing an effective and safe dose for various pediatric thresholds (ie, <5 kg, <10 kg) will be necessary. Finally, evaluating leflunomide's efficacy in patients with TTC7A deficiency may be confounded by the effects of concomitant immunodeficiency.

In this study, we have identified FDA-approved drugs that rescue TTC7A-deficiency phenotypes and orthogonally validated the potential therapies in zebrafish and patient-derived colonoids. We identified AKT activation as part of the pathobiology in TTC7A deficiency and proposed an alternative mechanism of action whereby leflunomide increases activated AKT and improves cellular fitness. The data presented here suggest that leflunomide is a repurposing candidate with potential to benefit patients with monogenic defects in TTC7A as well as in those in the broader IBD population suffering with apoptotic and/or stricturing intestinal disease. Based on these preclinical findings, leflunomide is a promising candidate to advance to clinical testing. Future investigation of the hits identified here could provide alternative therapeutic targets for TTC7A-deficiency and offer insight into the cellular functions of TTC7A.

Supplementary Material

Note: To access the supplementary material accompanying this article, visit the online version of *Gastroenterology* at www.gastrojournal.org, and at <https://doi.org/10.1053/j.gastro.2019.11.019>.

References

1. Avitzur Y, Guo C, Mastropaolo LA, et al. Mutations in tetratricopeptide repeat domain 7A result in a severe form of very early onset inflammatory bowel disease. *Gastroenterology* 2014;146:1028–1039.
2. Bigorgne AE, Farin HF, Lemoine R, et al. TTC7A mutations disrupt intestinal epithelial apicobasal polarity. *J Clin Invest* 2014;124:328–337.
3. Jardine S, Dhingani N, Muise AM. TTC7A: steward of intestinal health. *Cell Mol Gastroenterol Hepatol* 2019;7:555–570.
4. Lien R, Lin YF, Lai MW, et al. Novel mutations of the tetratricopeptide repeat domain 7A gene and phenotype/genotype comparison. *Front Immunol* 2017;8:1066.
5. Kammermeier J, Lucchini G, Pai SY, et al. Stem cell transplantation for tetratricopeptide repeat domain 7A deficiency: long-term follow-up. *Blood* 2016;128:1306–1308.
6. Blatch GL, Lassle M. The tetratricopeptide repeat: a structural motif mediating protein-protein interactions. *Bioessays* 1999;21:932–939.
7. Tan J, Brill JA. Cinderella story: PI4P goes from precursor to key signaling molecule. *Crit Rev Biochem Mol Biol* 2014;49:33–58.
8. Vaillancourt FH, Brault M, Pilote L, et al. Evaluation of phosphatidylinositol-4-kinase III α as a hepatitis C virus drug target. *J Virol* 2012;86:11595–11607.
9. Thakur PC, Davison JM, Stuckenholz C, et al. Dysregulated phosphatidylinositol signaling promotes endoplasmic-reticulum-stress-mediated intestinal mucosal injury and inflammation in zebrafish. *Dis Model Mech* 2014;7:93–106.
10. Breedveld F, Dayer J. Leflunomide: mode of action in the treatment of rheumatoid arthritis. *Ann Rheum Dis* 2000;59:841–849.
11. Zhang JH, Chung TD, Oldenburg KR. A simple statistical parameter for use in evaluation and validation of high throughput screening assays. *J Biomol Screen* 1999;4:67–73.
12. Varshney GK, Carrington B, Pei W, et al. A high-throughput functional genomics workflow based on CRISPR/Cas9-mediated targeted mutagenesis in zebrafish. *Nat Protoc* 2016;11:2357–2375.
13. Shi Y, Zhang Y, Zhao F, et al. Acetylcholine serves as a derepressor in loperamide-induced opioid-induced bowel dysfunction (OIBD) in zebrafish. *Sci Rep* 2014;4:5602.
14. Sato T, Stange DE, Ferrante M, et al. Long-term expansion of epithelial organoids from human colon, adenoma, adenocarcinoma, and Barrett's epithelium. *Gastroenterology* 2011;141:1762–1772.
15. Dekkers JF, Wiegerinck CL, de Jonge HR, et al. A functional CFTR assay using primary cystic fibrosis intestinal organoids. *Nat Med* 2013;19:939–945.
16. Chen G, Hou Z, Gulbranson DR, et al. Actin-myosin contractility is responsible for the reduced viability of dissociated human embryonic stem cells. *Cell Stem Cell* 2010;7:240–248.
17. Smith CE, Soti S, Jones TA, et al. Non-steroidal anti-inflammatory drugs are caspase inhibitors. *Cell Chem Biol* 2017;24:281–292.

18. Helms C, Pelsue S, Cao L, et al. The tetratricopeptide repeat domain 7 gene is mutated in flaky skin mice: a model for psoriasis, autoimmunity, and anemia. *Exp Biol Med (Maywood)* 2005;230:659–667.
19. Bassotti G, Antonelli E, Villanacci V, et al. Gastrointestinal motility disorders in inflammatory bowel diseases. *World J Gastroenterol* 2014;20:37–44.
20. Silverman E, Mouy R, Spiegel L, et al. Leflunomide or methotrexate for juvenile rheumatoid arthritis. *N Engl J Med* 2005;352:1655–1666.
21. Herrlinger KR, Diculescu M, Fellermann K, et al. Efficacy, safety and tolerability of vidofludimus in patients with inflammatory bowel disease: the ENTRANCE study. *J Crohns Colitis* 2013;7:636–643.
22. Leger DY, Liagre B, Beneytout JL. Low dose leflunomide activates PI3K/Akt signalling in erythroleukemia cells and reduces apoptosis induced by anticancer agents. *Apoptosis* 2006;11:1747–1760.
23. Holtmann MH, Gerts AL, Weinman A, et al. Treatment of Crohn's disease with leflunomide as second-line immunosuppression: a phase 1 open-label trial on efficacy, tolerability and safety. *Dig Dis Sci* 2008;53:1025–1032.
24. Autret-Leca E, Bensouda-Grimaldi L, Maurage C, et al. Upper gastrointestinal complications associated with NSAIDs in children. *Therapie* 2007;62:173–176.
25. Mortimore M, Florin TH. A role for B₁₂ in inflammatory bowel disease patients with suppurative dermatoses? An experience with high dose vitamin B₁₂ therapy. *J Crohns Colitis* 2010;4:466–470.
26. Ferrigno A, Berardo C, Di Pasqua LG, et al. Localization and role of metabotropic glutamate receptors subtype 5 in the gastrointestinal tract. *World J Gastroenterol* 2017;23:4500–4507.
27. Kim S, Chen J, Cheng T, et al. PubChem 2019 update: improved access to chemical data. *Nucleic Acids Res* 2019;47(D1):D1102–D1109.

Author names in bold designate shared co-first authorship.

Received June 21, 2019. Accepted November 5, 2019.

Correspondence

Address correspondence to: Aleixo Muise MD, PhD, 555 University Avenue, The Hospital for Sick Children, Toronto, Ontario, Canada, M5G 1X8. e-mail: aleixo.muise@utoronto.ca; fax: (416) 813-6531.

Acknowledgments

The authors thank all of the SickKids and Boston Children's Hospital patients and their families who consented and participated in this study as part of the NEOPICS (www.NEOPICS.org) and Helmsley VEOIBD (www.VEOIBD.org) consortia, as well as the health care professionals at The Hospital for Sick Children and Boston Children's Hospital who care for these patients with IBD (REB #1000024905, IRB-P00000529). We also thank Ramil Noche and the SickKids Zebrafish Genetics Core facility and Mark Jen for technical assistance. All zebrafish studies were performed via an Institutional Animal Care and Use Committee-approved protocol.

Author contributions: Sasha Jardine, Sierra Anderson, Jie Pan, and Stephen Babcock carried out all the experiments with supervision from Jay R. Thiagarajah and Aleixo M. Muise. Sasha Jardine and Aleixo M. Muise, with contributions from all authors, designed the outlined experiments and wrote the manuscript. All authors approved the final manuscript.

Conflicts of interest

The authors disclose no conflicts.

Funding

Aleixo M. Muise, Scott B. Snapper, Christoph Klein, and Daniel Kotlarz are supported by the Leona M. and Harry B. Helmsley Charitable Trust to study Very Early Onset Inflammatory Bowel Disease. Aleixo M. Muise is funded by a Canada Research Chair (Tier 1) in Pediatric Inflammatory Bowel Disease and a CIHR Foundation Grant. Aleixo M. Muise and Jay R. Thiagarajah are supported by the National Institute of Diabetes and Digestive and Kidney Diseases (NIDDK) (RC2DK118640). Christoph Klein and Daniel Kotlarz are supported by the Collaborative Research Consortium SFB1054 project A05. James J. Dowling is supported by CIHR Operating Grants. Jay R. Thiagarajah is funded by the NIDDK (K08DK113106), American Gastroenterological Association (Research Scholar Award), and Boston Children's Hospital (OFD Career Development Award).